

DESIGN AND CONSTRUCTION OF A CHOPPER DRIVEN 11.4GHZ TRAVELING WAVE RF GENERATOR

J. Haimson and B. Mecklenburg*

Haimson Research Corporation
4151 Middlefield Road • Palo Alto, CA 94303-4793

Abstract

This paper discusses design and construction features of a high power RF generator comprising a 5.7GHz chopping system and 11.4GHz high group velocity, traveling wave structures. The device is designed for operation with high current megavoltage beams and has been developed in support of the Relativistic Klystron High Gradient Accelerator program.^{1,2} The RF chopping system operates under immersed beam conditions with an axial magnetic field matched to the beam emittance and betatron resonance requirements so that the 11.4GHz RF current is maximized. The TW circuit shunt impedance was chosen to enable high levels of beam induced RF power to be generated without exceeding safe E-field values. The use of high group velocity structures having a short interaction region enabled an RF filling time of only 1050ps to be achieved, and thereby provided a broadband, phase and temperature insensitive circuit having fast response characteristics consistent with the intended 1000A 40ns beam pulse operation.

Introduction

An important design objective for the initial phase of this project was the generation of 200 to 250 MW of pulsed RF power at 11.424 GHz from each of two multiple cell output circuits driven by an RF modulated beam. The proposed electron source was a 1000A 3MeV induction linac having a beam pulse width and normalized emittance of approximately 40ns and 58π cm-mradian, respectively. Since the high RF power level was intended for short pulse excitation of high gradient accelerator (HGA) waveguides, emphasis was placed on the need (a) to achieve an RF phase and amplitude stability consistent with demonstrating narrow spectrum beam performance from the HGA, notwithstanding significant variations of the induction linac beam energy and position during the pulse, and (b) to design fast response RF generating structures so that the effective pulse width could be maximized.

To assist in meeting RF stability requirements, the initially considered dual chopping and free drift deflection techniques were discarded in favor of a single RF cavity chopper immersed in an axial magnetic field. With this concept, the maximized RF current is caused to have only a second order dependence on beam energy. This is achieved by using a quarter betatron wavelength chopper drift distance and by matching the beam emittance and deflection geometry axial magnetic field requirements so that the diameter of the deflected beam is maintained essentially constant during the semi-helical trajectories. The technique also minimizes emittance growth of the chopped beam, thereby enhancing beam transmission through the contiguously located 11.4GHz RF generating structures, and presents additional desirable RF power response characteristics, as discussed below.

A short traveling wave structure having a very high group velocity was the circuit of choice for this short pulse, high RF power application because of satisfactory prior S-band experience using relativistic bunched beams^{3,4} (at lower current levels), and because at 11.4GHz, large beam aperture geometry could be used to achieve RF steady state conditions within 1 nanosecond while retaining sufficiently high values of shunt impedance and circuit attenuation to ensure effective power transfer from the beam to the RF structure.

The insensitivity of the output coupler match to wide variations of beam loading, the flexibility of

*This work was supported in part by the U.S. DOE and by the Lawrence Livermore National Laboratory under W-7405-ENG-48.

dominant and higher order mode design parameters, and the favorably low values of E-field at high levels of RF power, as indicated in a following section, were additional compelling arguments that supported our decision to use TW structures for this high current application.

Principle of Operation

With reference to the beam centerline plan view illustrated in Figure 1, the B_z field immersed incoming electron beam is deflected in a horizontal plane by the 5.712 GHz TM₁₁₀ cavity causing the beam to describe semi-helical trajectories along the λ_B/4 drift space (refer Figure 2), and to scan in a vertical plane across the on-axis aperture of a water cooled collimator. (The plane of scanning at the collimator has been rotated 90° in Figure 1 for illustration purposes only.)

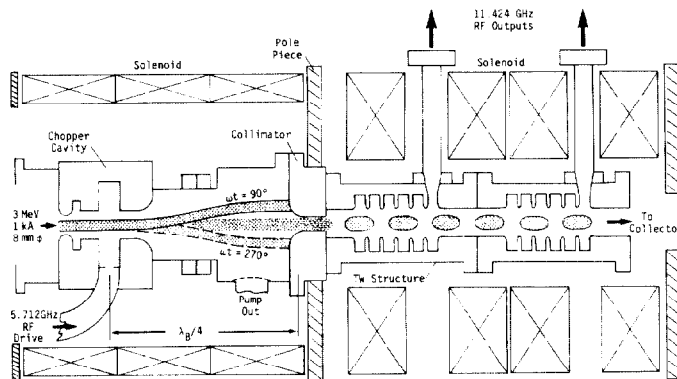


Figure 1. Centerline Layout of the Chopper Driven Traveling Wave RF Generator.

Thus, the 5.712 GHz spatially modulated dc beam incident on the collimator is transformed into a phase coherent, amplitude modulated beam at 11.424 GHz. By suitable selection of the circuit impedance and phase velocity, the induced E-fields, excited in the TW structures by this charge modulated beam, can be arranged to provide a specific loss of beam energy (and, therefore, generation of RF output power) for a given value of RF current.

RF Deflection System

In traversing the B_z field immersed RF deflector, axial electrons receiving a transverse momentum component (p_⊥) will trace out helical trajectories tangential to the centerline, recrossing it at a distance determined by the axial velocity β_{zc}. Thus, the maximum departure (2ρ) from the axis, as indicated in Figure 2, will occur after one-half helix rotation in a time interval given by πρ/β_{⊥c}, where ρ, the orbit radius, is given by the magnetic rigidity relationship B_zρ = 1704.5 β_⊥γ gauss-cm. Thus, the maximum deflection will occur at an axial distance beyond the deflector given by πρβ_{zc}/(β_{⊥c}) = 1704.5 πβ_zγ/B_z = λ_B/4, where λ_B is the betatron wavelength; and by substituting k_B = 2π/λ_B, the λ_B dependence on B_z and beam energy is given by the simple expression B_z = 3409 β_zγ k_B. Since this axial distance is independent of p_⊥, particles traversing the deflector at all RF phase angles (ωt) will arrive at z = λ_B/4 (the location of the chopping collimator) having each experienced half helix rotation but with different deflection values given by 2ρ sin ωt, as indicated in Figure 2' (for the phase convention of a particle crossing the midplane of the cavity at ωt = π/2 when the RF magnetic field is at a peak value).

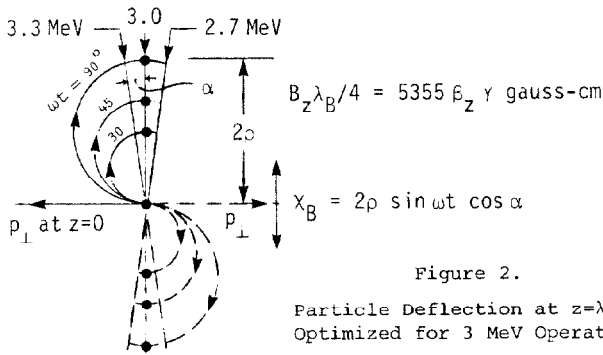


Figure 2.

Particle Deflection at $z=\lambda_B/4$
Optimized for 3 MeV Operation.

Unlike field free deflection systems, Figure 2 shows that for this $\lambda_B/4$ operating condition, at all RF phase angles, a 10 percent variation of beam energy, on either side of the optimum 3 MeV value, will have very little effect on the RF scanned beam with respect to intercepting edges of a collimating aperture; i.e., because the direction of the relative movements are orthogonal to each other, the 11.424 GHz current controlling parameter (χ), and therefore the RF power output, will be insensitive to beam energy fluctuations.

In analyzing the deflection of high current large emittance (ϵ) beams, it is necessary to consider radial space charge effects, azimuthal momentum imparted to the beam during traversal of the solenoid fringe fields, and emittance induced transverse momentum (especially for the near-axis orbits at entry to the chopper cavity). Unlike the above $\lambda_B/4$ B_z requirement, the axial magnetic field to match a given emittance is dependent on the beam diameter (d); thus, the chopper drift space geometry should be selected to ensure B_z compatibility and, preferably, to minimize emittance growth of the transmitted RF modulated beam. The design criteria for meeting these requirements is given by $k_B = \epsilon(d/2)^{-2}$ or $\lambda_B/4 = \pi d^2 / (8\epsilon)$. Thus, the distance between the chopper and the collimator can be established directly from a knowledge of the beam diameter and emittance. In evaluating the RF deflection system, it is also necessary to determine the maximum transverse deflection required to optimize the 11.4GHz harmonic content of the modulated beam. With this information, the desired transverse momentum (p_{\perp}) can be specified, since $\theta = p_{\perp}/p_z = 4\pi\rho/\lambda_B$, and the design of the chopper cavity can be completed.

The 11.424GHz RF current amplitude (a_2) dependence on the maximum beam deflection normalized to the collimator diameter ($2\rho/D$), is shown plotted in Figure 3 for collimator to beam diameter ratios of 1.0, 1.25 and 1.5.

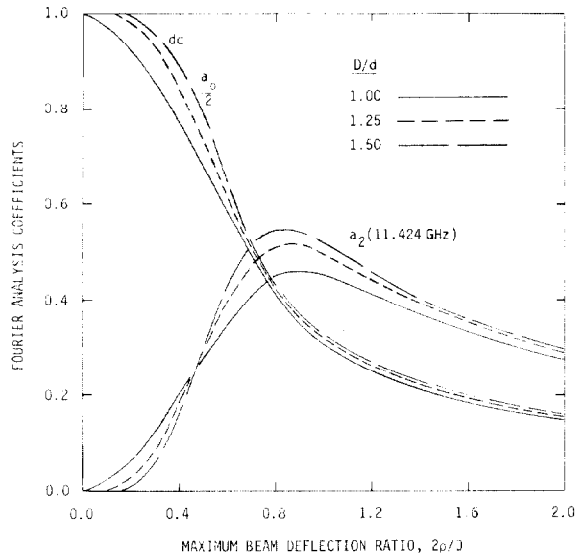


Figure 3. Fourier Analysis Coefficients of 5.712 GHz Chopped Beam versus Normalized Deflection.

This data was obtained from Fourier analyses of simulated charge distributions, in longitudinal phase space, by scanning beams of Gaussian ($d=4\sigma$) radial charge distribution across an on-axis aperture, using different beam diameters and increasing values of maximum deflection. The Figure 3 data reveals that for a given beam diameter there is a well defined optimum operating region in which the 11.424 GHz current is maximized at a specific value of beam deflection. Furthermore, it can be noted that these a_2 maxima are relatively insensitive to ± 4 percent variations of beam deflection (drive power variations of $\pm 8\%$); i.e., as well as having tolerance to beam energy variations, this RF generator will exhibit a drive power saturation characteristic similar to that of a klystron.

The $D/d=1.25$ curve of Figure 3 indicates that with a 10mm diameter collimator and a 1000A incident beam pulse, a peak deflection of 8.4 mm is required to maximize the 11.424 GHz current at 520 A; i.e., $p_{\perp} = 0.156$ MeV/c. The plotted data also suggests that higher RF currents can be achieved by trading system sensitivity for D/d ratio.

With one notable exception, the chopper cavity geometry and field computations were based on traditional design procedures,⁶ with a centerline symmetric H-field mode being most favored for this relatively large beam diameter application ($d/\lambda_0 = 0.15$). Unlike prior experience with linear accelerator systems, the deflected high current beam orbit studies suggested that the cavity impedance be selected to limit beam loading rather than to optimize the gain. Also, because of the short beam pulse, cavity coupling and Q values were chosen to limit transient effects. The dependence of beam loading and wall losses on cavity volume, for a constant value of $p_{\perp} = 0.156$ MeV/c, is shown in Figure 4 together with the design compromise adopted for the prototype cavity.

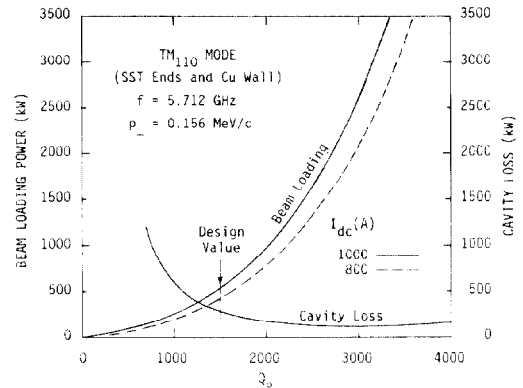


Figure 4. Beam Loading and Wall Loss Dependence on Q_0 for Varying Cavity Volume and Constant p_{\perp} .

Further details of the deflection induced variations of beam energy and phase, the chopper cavity beam loading, and the growth of beam emittance have been presented elsewhere;⁵ and the basic design parameters for the deflection system are summarized below.

Mode	TM ₁₁₀ Dipole
Cavity Center Frequency	5.712 GHz
Cavity Beam Apertures	16 mm
Quality Factor (Q_0)	1500
Matching Coefficient	2.5:1
Loaded Quality Factor (Q_L)	280
Dissipation in Cavity Walls	300 kW peak
Beam Loading at 800 A dc	450 kW peak
Loaded Cavity Peak H-Field	40.7 kA/m
Loaded Cavity Peak E-Field	17.8 MeV/m
Unloaded Cavity Peak E-Field	25.4 MeV/m
Unloaded Reflected Power	140 kW peak
Entry Beam Diameter	8 mm
Axial Magnetic Field	0.1245 T
$\lambda_B/4$ at 3 MeV	29.3 cm
Transverse Momentum	0.156 MeV/c
Beam Deflection at Collimator	8.4 mm
Collimator Diameter	10 mm

Generation of RF Power with TW Structures

Expressing the TW structure impedance as $Z=2P/(I_{RF}^2)$, the output power can be defined in conventional terms as $P = ZI_{RF}^2/2 = \Delta V I_{RF}/2$. From beam induced field considerations,³ and neglecting circuit dissipation for the present, with synchronous operation, the loss of beam energy (ΔV) in traversing the structure can be expressed as $\Delta V(\text{MeV})=(rL)\tau I_{RF}/4$, where (rL) is the TW shunt impedance of the overall structure in $M\Omega$, and τ is the circuit voltage attenuation in nepers. Thus, the RF output power can be expressed as $P = rL\tau I_{RF}^2/8$ or, alternatively, $P = (rL/16)(\omega T_F/Q)I_{RF}^2$; and for a $2\lambda_0$ long TW copper structure having the $v_p=c$ design parameters listed below, the power is given by $P(\text{MW})=\pi\lambda_0 r I_{RF}^2/(2Q v_g/c)=.0014I_{RF}^2$. With a uniform impedance circuit, these RF power expressions should be multiplied by $[(1-e^{-\tau})/\tau]^2$ to allow for circuit dissipation. A more rigorous analysis taking into account the use of high loss cavities at the beginning of the structure, and including phase orbit debunching and detuning effects, gives an RF output power value approximately 5 percent less than that obtained from the above simplified expressions.

In designing the prototype TW circuits, the output coupler E-field was arranged to be approximately the same as the WR90 output rectangular waveguide; e.g., at 11.4 GHz, the WR90 impedance is 410 Ω , giving an E-field of 45 MV/m at 250 MW. This field value influenced the selection of circuit length and aperture size (2a) in establishing r and v_g/c consistent with the desired ΔV and T_F values. Each structure comprises six, $v_p = c$, $2\pi/3$ mode cells including a side wall coupled, offset output cavity. The first three cells were constructed from low carbon 304 series SST, as a partial step toward the ultimate goal of an internally terminated circuit.³

The 1 ns filling time resulted in an extremely phase stable circuit, insensitive to normal variations of temperature and frequency, with operational derivatives of $\partial\phi/\partial T < 0.1^\circ/\text{C}$ and $\partial\phi/\partial f < 0.5^\circ/\text{MHz}$. The design parameters for these $v_p = c$ structures, as well as the tapered phase velocity (0.94c to 0.9c) circuit designed for the SHARK² project, are listed below.

Forward Traveling Wave Mode	TM ₀₁
Frequency	11.424 GHz
Phase Shift per Cavity.	120°
Electrical Length	720°
Output Cavity Beam Aperture	14.0 mm

	TW SHARK	CHOPPERTRON
Output Cavity Relative		
Phase Velocity (v_p/c)	0.90	1.00
Output Cavity Shunt Impedance (r)	23.5	41.5 $M\Omega/m$
Output Cavity Quality Factor (Q)	6300	7000
Output Cavity Avg. E-field at 250 MW.	37.5	45.0 MeV/m
Maximum Surface E-field at 250 MW (E_S)	140	145 MeV/m
Structure Impedance with Sync Beam (Z)	1800	2850 Ω
Approx. RF Current for 250 MW (I_{RF})	520	420 A
Harmonic Mean Group Velocity (v_g/c)	0.159	0.167
Total Filling Time (T_F)	1.01	1.05 ns

It can be noted that the output cavity average E-fields for these TW circuits are less than 50 MV/m at 250 MW, and that even with the adverse E_S/E_a ratio normally associated with large aperture (and $v_p < c$) geometry, the maximum surface E-field at this power level is not expected to exceed 150 MeV/m. (This can be compared to the 330 MeV/m design value for the SL4 klystron output cavity² and 230 MeV/m for typical HGA waveguides designed for a gradient of 100 MeV/m.)

Due to the large beam aperture, the $v_p=c$ structure has an HEM₁₁ lower branch dispersion curve with a forward wave propagation characteristic and a π cut-off frequency at approximately 13.8 GHz. (This π -mode frequency is reduced by approximately 80 MHz with the $v_p < c$ cavities used for SHARK.) For beam energies over the working range 3 to 0.6 MeV, the dispersion curve phase velocity intercepts straddle the π -mode from $5\pi/6$ to the first backward space

harmonic frequency at $7\pi/6$ (≈ 13.7 GHz), i.e., over a region conducive to BBU because of high (r/Q) values and phase slips of 10° to 30° per cell. Thus, for applications requiring a multiple array of these broadband TW structures, a large reduction of the HEM₁₁ field intensities will be necessary,⁵ using design techniques that emphasize absorption and differential extraction⁷ rather than stagger tuning⁸ or progressive stopband⁹ procedures.

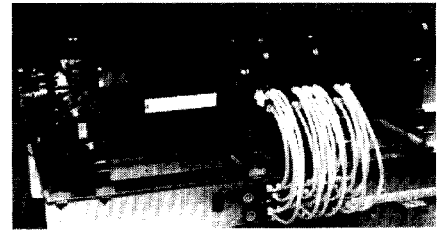
Applying a 30 percent contingency factor to the predicted $5/\pi$ emittance growth caused by the chopper gives a normalized emittance of $\beta\gamma\epsilon=120\pi$ cm-mradian for the RF modulated beam. Thus, with a nominal 9 mm beam diameter, the B_z required for the TW structures is 0.21T (60 percent greater than the deflection system). With this configuration, the TW structures have an admittance 2.4 times greater than the beam emittance. The solenoids were constructed with water-cooled, counter-wound pancake coils and assembled with a stacking technique to give cancellation of internal longitudinal current vectors.

The Figure 5 views show the chopper driven RF generator assembly before and after installation of the externally shielded, water-cooled solenoid windings.

Figure 5.
(a)
Choppertron Centerline Assembly Showing the Dual WR90 Output Arms



(b)
Overall System Showing Input RF Flange and Solenoid Assemblies



Initial test results of the tapered phase velocity TW structure designed for SHARK and subsequently installed on the SL4 klystron have been reported in a companion paper,² and tests at LLNL on the chopper driven RF generator are being planned for later this year.

Acknowledgements

The authors would like to thank D. Prono (LLNL) for drawing our attention to the magnitude of induction linac beam variations, R. Miller (SLAC) for helpful discussions on emittance growth, and colleagues at HRC for their dedicated efforts during the design study and construction phases of this project.

References

1. A.M. Sessler and S.S. Yu, "Relativistic Klystron Two-Beam Accelerator," *Phys. Rev. Lett.* **58**, p. 2439, 1987.
2. M.A. Allen, et al., 1989 PAC IEEE Conference Records 89CH2669-0, also SLAC PUB-4861, Feb. 1989.
3. J. Haimson, "Absorption and Generation of Radio-Frequency Power in Electron Linear Accelerator Systems," *Nucl. Instr. & Meth.*, **33** No. 1, p. 93, 1965.
4. D.G. Dow, et al., "Pulse Compression using Linear Accelerator Techniques," Conference on Electron Device Research, Cornell University, June 1964.
5. "Chopper Driven Traveling Wave Relativistic Klystron Design Report No. HRC-774, Jan. 1983.
6. J. Haimson, "Optimization Criteria for SW Transverse Magnetic Deflection Cavities," Los Alamos, LA Report 3609, Oct. 1966.
7. J. Haimson and B. Mecklenburg, "A CW Non-Synchronous Traveling Wave Structure for a 300 MeV Pulse Stretcher Ring," 1987 PAC IEEE Conf. Rec. 87CH2387-9, p. 1919.
8. *Linear Accelerators*, Eds. P. Lapostolle and A. Septier, p. 216, North Holland Publishing Co., Amsterdam, 1970.
9. *Ibid*, p. 450.